MODELING AND CIRCUIT-BASED SIMULATION OF PHOTOVOLTAIC ARRAYS

M. G. Villalva, J. R. Gazoli, E. Ruppert F.
University of Campinas - UNICAMP, Brazil
mvillalva@gmail.com, gazoli@gmail.com, ruppert@fee.unicamp.br

Abstract—**This paper presents an easy and accurate method of modeling photovoltaic arrays. The method is used to obtain the parameters of the array model using information from the datasheet. The photovoltaic array model can be simulated with any circuit simulator. The equations of the model are presented in details and the model is validated with experimental data. Finally, simulation examples are presented. This paper is useful for power electronics designers and researchers who need an effective and straightforward way to model and simulate photovoltaic arrays.**

Keywords—**Array, circuit, equivalent, model, modeling, photovoltaic, PV, simulation.**

I. INTRODUCTION

A photovoltaic system converts sunlight into electricity. The basic device of a photovoltaic system is the photovoltaic cell. Cells may be grouped to form panels or modules. Panels can be grouped to form large photovoltaic arrays. The term *array* is usually employed to describe a photovoltaic panel (with several cells connected in series and/or parallel) or a group of panels. Most of time one are interested in modeling photovoltaic panels, which are the commercial photovoltaic devices. This paper focuses on modeling photovoltaic modules or panels composed of several basic cells. The term *array* used henceforth means any photovoltaic device composed of several basic cells. In the Appendix at the end of this paper there are some explanations about how to model and simulate large photovoltaic arrays composed of several panels connected in series or in parallel.

The electricity available at the terminals of a photovoltaic array may directly feed small loads such as lighting systems and DC motors. Some applications require electronic converters to process the electricity from the photovoltaic device. These converters may be used to regulate the voltage and current at the load, to control the power flow in grid-connected systems and mainly to track the maximum power point (MPP) of the device.

Photovoltaic arrays present a nonlinear *I-V* characteristic with several parameters that need to be adjusted from experimental data of practical devices. The mathematical model of the photovoltaic array may be useful in the study of the dynamic analysis of converters, in the study of maximum power point tracking (MPPT) algorithms and mainly to simulate the photovoltaic system and its components using circuit simulators.

This text presents in details the equations that form the the *I-V* model and the method used to obtain the parameters of the equation. The aim of this paper is to provide the reader with all necessary information to develop photovoltaic array models and circuits that can be used in the simulation of power converters for photovoltaic applications.

II. MODELING OF PHOTOVOLTAIC ARRAYS

A. Ideal photovoltaic cell

Fig. 1 shows the equivalent circuit of the ideal photovoltaic cell. The basic equation from the theory of semiconductors [1] that mathematically describes the *I-V* characteristic of the ideal photovoltaic cell is:

$$I = I_{\mathrm{pv,cell}} - \underbrace{I_{0,\mathrm{cell}} \left[\exp\left(\frac{qV}{akT} \right) - 1 \right]}_{I_{\mathrm{d}}} \qquad (1)$$

where $I_{\mathrm{pv,cell}}$ is the current generated by the incident light (it is directly proportional to the Sun irradiation), I_{d} is the Shockley diode equation, $I_{0,\mathrm{cell}}$ [A] is the reverse saturation or leakage current of the diode [A], q is the electron charge [$1.60217646 \cdot 10^{-19}$C], k is the Boltzmann constant [$1.3806503 \cdot 10^{-23}$J/K], T [K] is the temperature of the *p-n* junction, and a is the diode ideality constant. Fig. 2 shows the *I-V* curve originated from (1).

B. Modeling the photovoltaic array

The basic equation (1) of the elementary photovoltaic cell does not represent the *I-V* characteristic of a practical photovoltaic array. Practical arrays are composed of several connected photovoltaic cells and the observation of the characteristics at the terminals of the photovoltaic array requires the inclusion of additional parameters to the basic equation [1]:
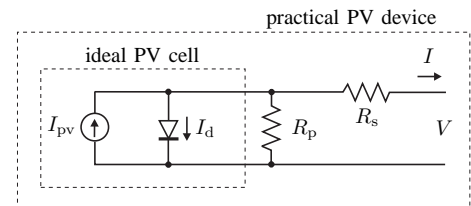

Fig. 1. Single-diode model of the theoretical photovoltaic cell and equivalent circuit of a practical photovoltaic device including the series and parallel resistances.
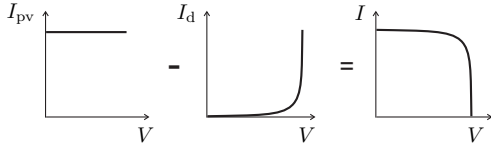
Fig. 2. Characteristic I-V curve of the photovoltaic cell. The net cell current I is composed of the light-generated current I_{pv} and the diode current I_d.
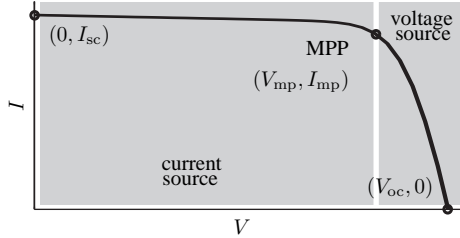

Fig. 3. Characteristic I-V curve of a practical photovoltaic device and the three *remarkable points*: short circuit $(0, I_{sc})$, maximum power point (V_{mp}, I_{mp}) and open-circuit $(V_{oc}, 0)$.

$$I = I_{pv} - I_0 \left[\exp \left(\frac{V + R_s I}{V_t a} \right) - 1 \right] - \frac{V + R_s I}{R_p} \qquad (2)$$

where I_{pv} and I_0 are the photovoltaic and saturation currents of the array and $V_t = N_s k T / q$ is the thermal voltage of the array with N_s cells connected in series. Cells connected in parallel increase the current and cells connected in series provide greater output voltages. If the array is composed of N_p parallel connections of cells the photovoltaic and saturation currents may be expressed as: $I_{pv} = I_{pv,cell} N_p$, $I_0 = I_{0,cell} N_p$. In (2) R_s is the equivalent series resistance of the array and R_p is the equivalent parallel resistance. This equation originates the I-V curve seen in Fig. 3, where three *remarkable points* are highlighted: short circuit $(0, I_{sc})$, maximum power point (V_{mp}, I_{mp}) and open-circuit $(V_{oc}, 0)$.

Eq. (2) describes the single-diode model presented in Fig. 1. Some authors have proposed more sophisticated models that present better accuracy and serve for different purposes. For example, in [2]–[6] an extra diode is used to represent the effect of the recombination of carriers. In [7] a three-diode model is proposed to include the influence of effects which are not considered by the previous models. For simplicity the single-diode model of Fig. 1 is studied in this paper. This model offers a good compromise between simplicity and accuracy [8] and has been used by several authors in previous works, sometimes with simplifications but always with the basic structure composed of a current source and a parallel diode [9]–[23]. The simplicity of the single-diode model with the method for adjusting the parameters and the improvements proposed in this paper make this model perfect for power electronics designers who are looking for an easy and effective model for the simulation of photovoltaic devices with power converters.

Manufacturers of photovoltaic arrays, instead of the I-V equation, provide only a few experimental data about electrical and thermal characteristics. Unfortunately some of the parameters required for adjusting photovoltaic array models cannot be found in the manufacturers's data sheets, such as the light-generated or photovoltaic current, the series and shunt resistances, the diode ideality constant, the diode reverse saturation current, and the bandgap energy of the semiconductor. All photovoltaic array datasheets bring basically the following information: the nominal open-circuit voltage $V_{oc,n}$, the nominal short-circuit current $I_{sc,n}$, the voltage at the maximum power point V_{mp}, the current at the maximum power point I_{mp}, the open-circuit voltage/temperature coefficient K_V, the short-circuit current/temperature coefficient K_I, and the maximum experimental peak output power $P_{max,e}$. This information is always provided with reference to the nominal or standard test conditions (STC) of temperature and solar irradiation. Some manufacturers provide I-V curves for several irradiation and temperature conditions. These curves make easier the adjustment and the validation of the desired mathematical I-V equation. Basically this is all the information one can get from datasheets of photovoltaic arrays.

Electric generators are generally classified as current or voltage sources. The practical photovoltaic device presents an hybrid behavior, which may be of current or voltage source depending on the operating point, as shown in Fig. 3. The practical photovoltaic device has a series resistance R_s whose influence is stronger when the device operates in the voltage source region, and a parallel resistance R_p with stronger influence in the current source region of operation. The R_s resistance is the sum of several structural resistances of the device [24]. The R_p resistance exists mainly due to the leakage current of the *p-n* junction and depends on the fabrication method of the photovoltaic cell. The value of R_p is generally high and some authors [11]–[14], [17], [18], [25]–[28] neglect this resistance to simplify the model. The value of R_s is very low and sometimes this parameter is neglected too [26], [29]–[31].

The I-V characteristic of the photovoltaic device shown in Fig. 3 depends on the internal characteristics of the device (R_s, R_p) and on external influences such as irradiation level and temperature. The amount of incident light directly affects the generation of charge carriers and consequently the current generated by the device. The light-generated current (I_{pv}) of the elementary cells, without the influence of the series and parallel resistances, is difficult to determine. Datasheets only inform the nominal short-circuit current ($I_{sc,n}$), which is the maximum current available at the terminals of the practical device. The assumption $I_{sc} \approx I_{pv}$ is generally used in photovoltaic models because in practical devices the series resistance is low and the parallel resistance is high. The light-generated current of the photovoltaic cell depends linearly on the solar irradiation and is also influenced by the temperature according to the following equation [19], [32]–[34]:

$$I_{pv} = (I_{pv,n} + K_I \Delta_T) \frac{G}{G_n} \qquad (3)$$

where $I_{pv,n}$ $[A]$ is the light-generated current at the nominal condition (usually $25\,°C$ and $1000 W/m^2$), $\Delta_T = T - T_n$

(being T and T_n the actual and nominal temperatures [K]), G [W/m^2] is the irradiation on the device surface, and G_n is the nominal irradiation.

The diode saturation current I_0 and its dependence on the temperature may be expressed by (4) [32], [33], [35]–[38]:

$$I_0 = I_{0,n} \left(\frac{T_n}{T}\right)^3 \exp\left[\frac{qE_g}{ak}\left(\frac{1}{T_n} - \frac{1}{T}\right)\right] \quad (4)$$

where E_g is the bandgap energy of the semiconductor ($E_g \approx$ 1.12 eV for the polycrystalline Si at 25 °C [11], [32]), and $I_{0,n}$ is the nominal saturation current:

$$I_{0,n} = \frac{I_{sc,n}}{\exp\left(\frac{V_{oc,n}}{aV_{t,n}}\right) - 1} \quad (5)$$

with $V_{t,n}$ being the thermal voltage of N_s series-connected cells at the nominal temperature T_n.

The saturation current I_0 of the photovoltaic cells that compose the device depend on the saturation current density of the semiconductor (J_0, generally given in [A/cm^2]) and on the effective area of the cells. The current density J_0 depends on the intrinsic characteristics of the photovoltaic cell, which depend on several physical parameters such as the coefficient of diffusion of electrons in the semiconductor, the lifetime of minority carriers, the intrinsic carrier density, and others [7]. This kind of information is not usually available for commercial photovoltaic arrays. In this paper the nominal saturation current $I_{0,n}$ is indirectly obtained from the experimental data through (5), which is obtained by evaluating (2) at the nominal open-circuit condition, with $V = V_{oc,n}$, $I = 0$, and $I_{pv} \approx I_{sc,n}$.

The value of the diode constant a may be arbitrarily chosen. Many authors discuss ways to estimate the correct value of this constant [8], [11]. Usually $1 \leq a \leq 1.5$ and the choice depends on other parameters of the I-V model. Some values for a are found in [32] based on empirical analysis. As [8] says, there are different opinions about the best way to choose a. Because a expresses the degree of ideality of the diode and it is totally empirical, any initial value of a can be chosen in order to adjust the model. The value of a can be later modified in order to improve the model fitting if necessary. This constant affects the curvature of the I-V characteristic and varying a can slightly improve the model accuracy.

C. Improving the model

The photovoltaic model described in the previous section can be improved if equation (4) is replaced by:

$$I_0 = \frac{I_{sc,n} + K_I \Delta_T}{\exp\left(\frac{V_{oc,n} + K_V \Delta_T}{aV_t}\right) - 1} \quad (6)$$

This modification aims to match the open-circuit voltages of the model with the experimental data for a very large range of temperatures. Eq. (6) is obtained from (5) by including in the equation the current and voltage coefficients K_V and K_I. The saturation current I_0 is strongly dependent on the temperature and (6) proposes a different approach to express the dependence of I_0 on the temperature so that the net effect of the temperature is the linear variation of the open-circuit voltage according the the practical voltage/temperature coefficient. This equation simplifies the model and cancels the model error at the vicinities of the open-circuit voltages and consequently at other regions of the I-V curve.

The validity of the model with this new equation has been tested through computer simulation and through comparison with experimental data. One interesting fact about the correction introduced with (6) is that the coefficient K_V from the manufacturer's datasheet appears in the equation. The voltage/temperature coefficient K_V brings important information necessary to achieve the best possible I-V curve fitting for temperatures different of the nominal value.

If one wish to keep the traditional equation (4) [32], [33], [35]–[38], instead of using (6), it is possible to obtain the best value of E_g for the model so that the open-circuit voltages of the model are matched with the open-circuit voltages of the real array in the range $T_n < T < T_{max}$. By equaling (4) and (6) and solving for E_g at $T = T_{max}$ one gets:

$$E_g = -\ln\left[\frac{\left(\frac{I_{sc,Tmax}}{I_{0,n}}\right)\left(\frac{T_n}{T_{max}}\right)^3}{\exp\left(\frac{qV_{oc,Tmax}}{aN_skT_{max}}\right) - 1}\right] \cdot \\ \cdot \frac{akT_nT_{max}}{q(T_n - T_{max})} \quad (7)$$

where $I_{sc,Tmax} = I_{sc,n} + K_I\Delta_T$ and $V_{oc,Tmax} = V_{oc,n} + K_V\Delta_T$, with $\Delta_T = T_{max} - T_n$.

D. Adjusting the model

Two parameters remain unknown in (2), which are R_s and R_p. A few authors have proposed ways to mathematically determine these resistances. Although it may be useful to have a mathematical formula to determine these unknown parameters, any expression for R_s and R_p will always rely on experimental data. Some authors propose varying R_s in an iterative process, incrementing R_s until the I-V curve visually fits the experimental data and then vary R_p in the same fashion. This is a quite poor and inaccurate fitting method, mainly because R_s and R_p may not be adjusted separately if a good I-V model is desired.

This paper proposes a method for adjusting R_s and R_p based on the fact that there is an only pair $\{R_s, R_p\}$ that warranties that $P_{max,m} = P_{max,e} = V_{mp}I_{mp}$ at the (V_{mp}, I_{mp}) point of the I-V curve, i.e. the maximum power calculated by the I-V model of (2), $P_{max,m}$, is equal to the maximum experimental power from the datasheet, $P_{max,e}$, at the maximum power point (MPP). Conventional modeling methods found in the literature take care of the I-V curve but forget that the P-V (power vs. voltage) curve must match the experimental data too. Works like [26], [39] gave attention to the necessity of matching the power curve but with different or simplified models. In [26], for example, the series resistance of the array model is neglected.

The relation between R_s and R_p, the only unknowns of (2), may be found by making $P_{max,m} = P_{max,e}$ and solving the resulting equation for R_s, as (8) and (9) show.
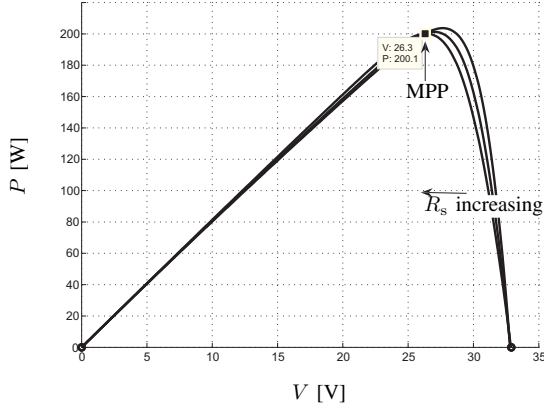
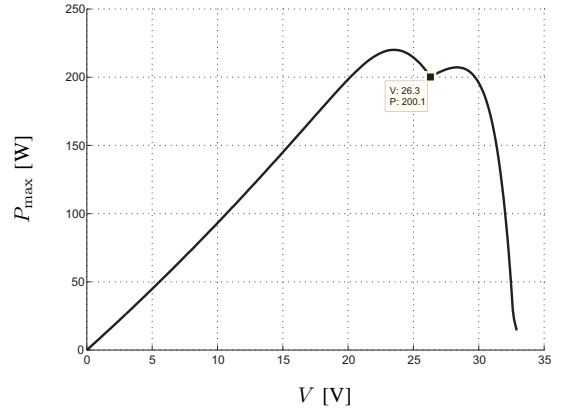Fig. 4. P-V curves plotted for different values of R_s and R_p.

Fig. 5. $P_\mathrm{max,m}$ vs. V for several values of $R_\mathrm{s} > 0$.

$$P_\mathrm{max,m} =$$
$$= V_\mathrm{mp}\left\{ I_\mathrm{pv} - I_0\left[\exp\left(\frac{q}{kT}\frac{V_\mathrm{mp} + R_\mathrm{s}I_\mathrm{mp}}{aN_\mathrm{s}}\right) - 1\right] \right. \quad - \quad (8)$$
$$\left. -\frac{V_\mathrm{mp} + R_s I_\mathrm{mp}}{R_\mathrm{p}} \right\} = P_\mathrm{max,e}$$

$$R_\mathrm{p} = V_\mathrm{mp}(V_\mathrm{mp} + I_\mathrm{mp}R_\mathrm{s})/$$
$$\left\{ V_\mathrm{mp}I_\mathrm{pv} - V_\mathrm{mp}I_0\exp\left[\frac{(V_\mathrm{mp} + I_\mathrm{mp}R_\mathrm{s})}{N_\mathrm{s}a}\frac{q}{kT}\right] + \quad (9) \right.$$
$$\left. +V_\mathrm{mp}I_0 - P_\mathrm{max,e} \right\}$$

Eq. (9) means that for any value of R_s there will be a value of R_p that makes the mathematical I-V curve cross the experimental $(V_\mathrm{mp}, I_\mathrm{mp})$ point.

E. Iterative solution of R_s and R_p

The goal is to find the value of R_s (and hence R_p) that makes the peak of the mathematical P-V curve coincide with the experimental peak power at the $(V_\mathrm{mp}, I_\mathrm{mp})$ point. This requires several iterations until $P_\mathrm{max,m} = P_\mathrm{max,e}$.

In the iterative process R_s must be slowly incremented starting from $R_\mathrm{s} = 0$. Adjusting the P-V curve to match the experimental data requires finding the curve for several values of R_s and R_p. Actually plotting the curve is not necessary, as only the peak power value is required. Figs. 4 and 6 illustrate how this iterative process works. In Fig. 4 as R_s increases the P-V curve moves to the left and the peak power ($P_\mathrm{max,m}$) goes towards the experimental MPP. Fig. 5 shows the contour drawn by the peaks of the power curves for several values of R_s (this example uses the parameters of the Kyocera KC200GT solar array [40]). For every P-V curve of Fig. 4 there is a corresponding I-V curve in Fig. 6. As expected from (9), all I-V curves cross the desired experimental MPP point at $(V_\mathrm{mp}, I_\mathrm{mp})$.

Plotting the P-V and I-V curves requires solving (2) for $I \in [0, I_\mathrm{sc,n}]$ and $V \in [0, V_\mathrm{oc,n}]$. Eq. (2) does not have a direct solution because $I = f(V, I)$ and $V = f(I, V)$. This transcendental equation must be solved by a numerical method and this imposes no difficulty. The I-V points are easily obtained by numerically solving $g(V, I) = I - f(V, I) = 0$ for a set of V values and obtaining the corresponding set of I points. Obtaining the P-V points is straightforward.
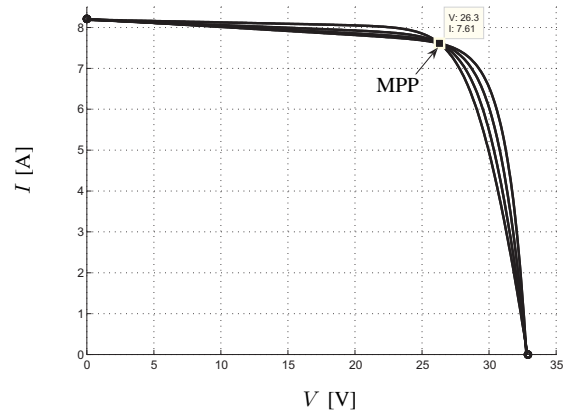

Fig. 6. I-V curves plotted for different values of R_s and R_p.

The iterative method gives the solution $R_\mathrm{s} = 0.221\,\Omega$ for the KC200GT array. Fig. 5 shows a plot of $P_\mathrm{max,m}$ as a function of V for several values of R_s. There is an only point, corresponding to a single value of R_s, that satisfies the imposed condition $P_\mathrm{max,m} = V_\mathrm{mp}I_\mathrm{mp}$ at the $(V_\mathrm{mp}, I_\mathrm{mp})$ point. Fig. 7 shows a plot of $P_\mathrm{max,m}$ as a function of R_s for $I = I_\mathrm{mp}$ and $V = V_\mathrm{mp}$. This plot shows that $R_\mathrm{s} = 0.221\,\Omega$ is the desired solution, in accordance with the result of the iterative method. This plot may be an alternative way for graphically finding the solution for R_s.
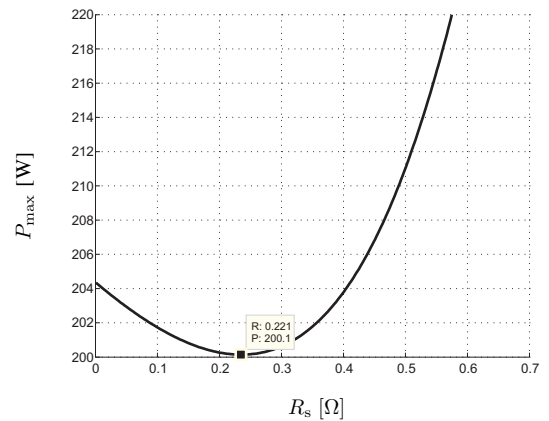

Fig. 7. $P_\mathrm{max} = f(R_\mathrm{s})$ with $I = I_\mathrm{mp}$ and $V = V_\mathrm{mp}$.
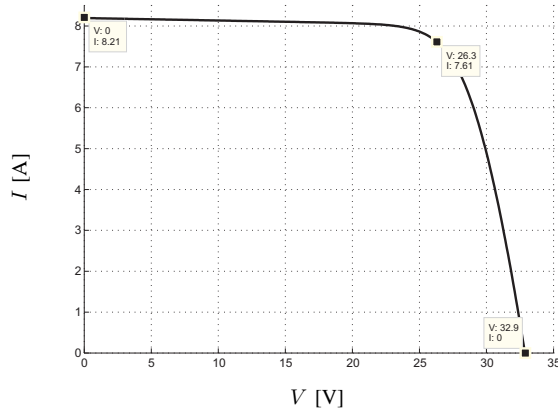
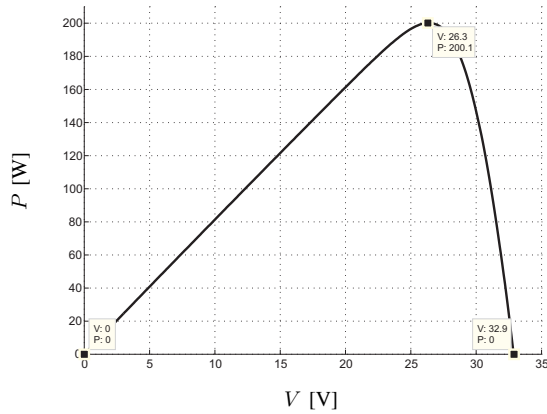Fig. 8. *I-V* curve adjusted to three *remarkable points*.

Fig. 9. *P-V* curve adjusted to three *remarkable points*.

Figs. 8 and 9 show the *I-V* and *P-V* curves of the KC200GT photovoltaic array adjusted with the proposed method. The model curves *exactly* match with the experimental data at the three *remarkable points* provided by the datasheet: short circuit, maximum power, and open circuit. Table I shows the experimental parameters of the array obtained from the datasheeet and Table II shows the adjusted parameters and model constants.

F. Further improving the model

The model developed in the preceding sections may be further improved by taking advantage of the iterative solution of R_s and R_p. Each iteration updates R_s and R_p towards the best model solution, so equation (10) may be introduced in the model.

TABLE I
Parameters of the KC200GT solar
array at 25 °C, 1.5AM, 1000 W/m².

I_{mp}	7.61 A
V_{mp}	26.3 V
$P_{max,e}$	200.143 W
I_{sc}	8.21 A
V_{oc}	32.9 V
K_V	−0.1230 V/K
K_I	0.0032 A/K
N_s	54

TABLE II
Parameters of the adjusted model of the
KC200GT solar array at nominal
operating conditions.

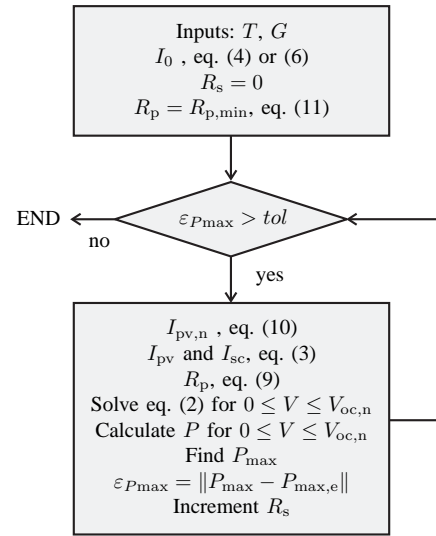|	
I_{mp}	7.61 A
V_{mp}	26.3 V
$P_{max,m}$	200.143 W
I_{sc}	8.21 A
V_{oc}	32.9 V
$I_{0,n}$	$9.825 \cdot 10^{-8}$ A
I_{pv}	8.214 A
a	1.3
R_p	415.405 Ω
R_s	0.221 Ω

Fig. 10. Algorithm of the method used to adjust the *I-V* model.

$$I_{pv,n} = \frac{R_p + R_s}{R_p} I_{sc,n} \qquad (10)$$

Eq. (10) uses the resistances R_s and R_p to determine $I_{pv} \neq I_{sc}$. The values of R_s and R_p are initially unknown but as the solution of the algorithm is refined along successive iterations the values of R_s and R_p tend to the best solution and (10) becomes valid and effectively determines the light-generated current I_{pv} taking in account the influence of the series and parallel resistances of the array. Initial guesses for R_s and R_p are necessary before the iterative process starts. The initial value of R_s may be zero. The initial value of R_p may be given by:

$$R_{p,min} = \frac{V_{mp}}{I_{sc,n} - I_{mp}} - \frac{V_{oc,n} - V_{mp}}{I_{mp}} \qquad (11)$$

Eq. (11) determines the minimum value of R_p, which is the slope of the line segment between the short-circuit and the maximum-power *remarkable points*. Although R_p is still unknown, it surely is greater than $R_{p,min}$ and this is a good initial guess.

G. Modeling algorithm

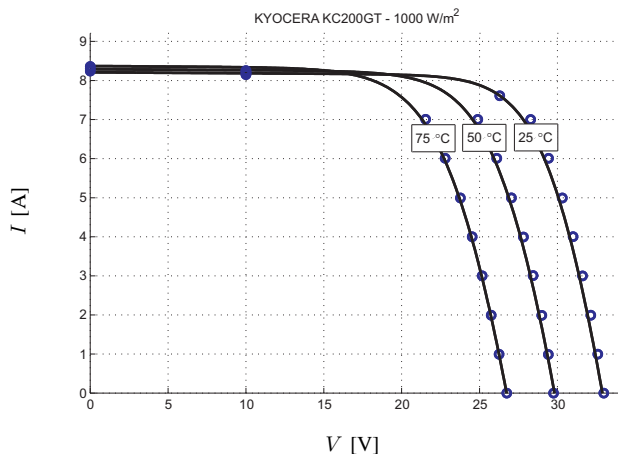The simplified flowchart of the iterative modeling algorithm is illustrated in Fig. 10.

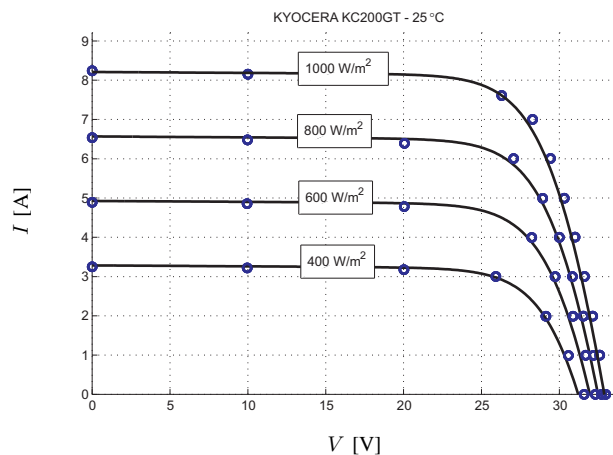Fig. 11. *I-V* model curves and experimental data of the KC200GT solar array at different temperatures, 1000 W/m².

Fig. 12. *I-V* model curves and experimental data of the KC200GT solar array at different irradiations, 25 °C.

III. VALIDATING THE MODEL

As Tables I and II and Figs. 8 and 9 have shown, the developed model and the experimental data are exactly matched at the nominal *remarkable points* of the *I-V* curve and the experimental and mathematical maximum peak powers coincide. The objective of adjusting the mathematical *I-V* curve at the three *remarkable points* was successfully achieved.

In order to test the validity of the model a comparison with other experimental data (different of the nominal *remarkable points*) is very useful. Fig. 11 shows the mathematical *I-V* curves of the KC200GT solar panel plotted with the experimental data at three different temperature conditions. Fig. 12 shows the *I-V* curves at different irradiations. The circular markers in the graphs represent experimental (V, I) points extracted from the datasheet. Some points are not exactly matched because the model is not perfect, although it is exact at the *remarkable points* and sufficiently accurate for other points. The model accuracy may be slightly improved by running more iterations with other values of the constant a, without modifications in the algorithm.

Fig. 13 shows the mathematical *I-V* curves of the Solarex MSX60 solar panel [41] plotted with the experimental data at two different temperature conditions. Fig. 14 shows the *P-V* curves obtained at the two temperatures. The circular markers in the graphs represent experimental (V, I) and (V, P) points extracted from the datasheet. Fig. 14 proves that the model accurately matches with the experimental data both in the current and power curves, as expected.

IV. SIMULATION OF THE PHOTOVOLTAIC ARRAY

The photovoltaic array can be simulated with an equivalent circuit model based on the photovoltaic model of Fig. 1. Two simulation strategies are possible.

Fig. 15 shows a circuit model using one current source (I_m) and two resistors $(R_s$ and $R_p)$. This circuit can be implemented with any circuit simulator. The value of the model current I_m is calculated by the computational block that has V, I, I_0 and I_{pv} as inputs. I_0 is obtained from (4) or (6) and I_{vp} is obtained from (3). This computational
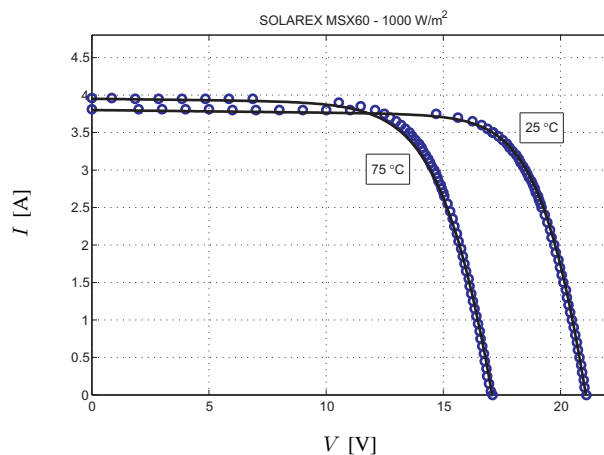

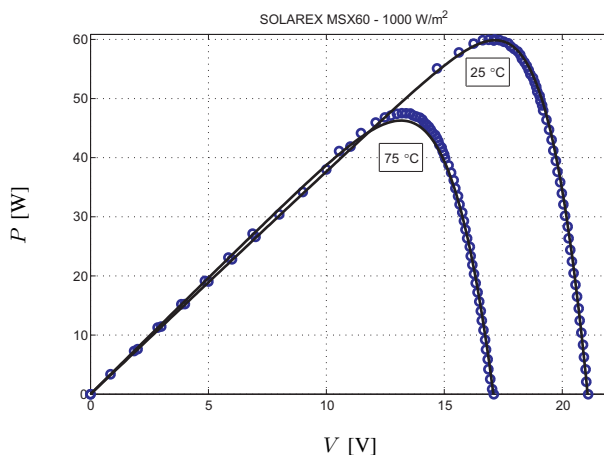Fig. 13. *I-V* model curves and experimental data of the MSX60 solar array at different temperatures, 1000 W/m².

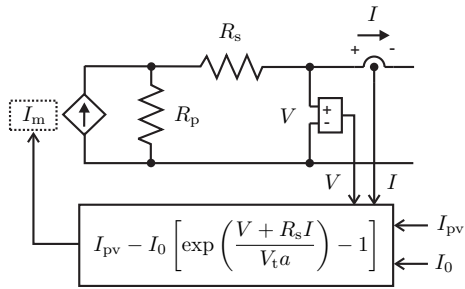Fig. 14. *P-V* model curves and experimental data of the MSX60 solar array at different temperatures, 1000 W/m².

Fig. 15. Photovoltaic array model circuit with a controlled current source, equivalent resistors and the equation of the model current (I_m).

Fig. 16. Photovoltaic array model circuit with a controlled current source and a computational block that solves the I-V equation.

block may be implemented with any circuit simulator able to evaluate math functions.

Fig. 16 shows another circuit model composed of only one current source. The value of the current is obtained by numerically solving the I-V equation. For every value of V a corresponding I that satisfies the I-V equation (2) is obtained. The solution of (2) can be implemented with a numerical method in any circuit simulator that accepts embedded programming. This is the simulation strategy proposed in [42].

Other authors have proposed circuits for simulating photovoltaic arrays that are based on simplified equations and/or require lots of computational effort [12], [26], [27], [43]. In [12] a circuit-based photovoltaic model is composed of a current source driven by an intricate and inaccurate equation where the parallel resistance is neglected. In [26] an intricate PSpice-based simulation was presented, where the I-V equation is numerically solved within the PSpice software. Although interesting, the approach found in [26] is excessively elaborated and concerns the simplified photovoltaic model without the series resistance. In [27] a simple circuit-based photovoltaic model is proposed where the parallel resistance is neglected. In [43] a circuit-based model was proposed based on the piecewise approximation of the I-V curve. Although interesting and relatively simple, this method [43] does not provide a solution to find the parameters of the I-V equation and the circuit model requires many components.

Figs. 17 and 18 show the photovoltaic model circuits implemented with MATLAB/SIMULINK (using the SymPowerSystems blockset) and PSIM using the simulation strategy of Fig. 15. Both circuit models work perfectly and may be used in the simulation of power electronics converters for photovoltaic systems. Figs. 19 and 20 show the I-V curves of the Solarex MSX60 solar panel [41] simulated with the MATLAB/SIMULINK and PSIM circuits.

V. CONCLUSION

This paper has analyzed the development of a method for the mathematical modeling of photovoltaic arrays. The objective of the method is to fit the mathematical I-V equation to the experimental *remarkable points* of the I-V curve of the practical array. The method obtains the parameters of the I-V equation by using the following nominal information from the array datasheet: open-circuit voltage, short-circuit current, maximum output power, voltage and current at the maximum power point, current/temperature and
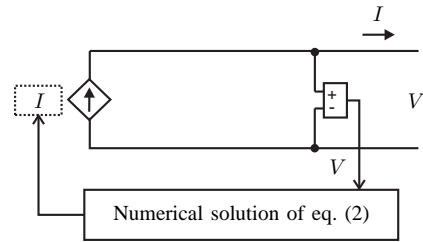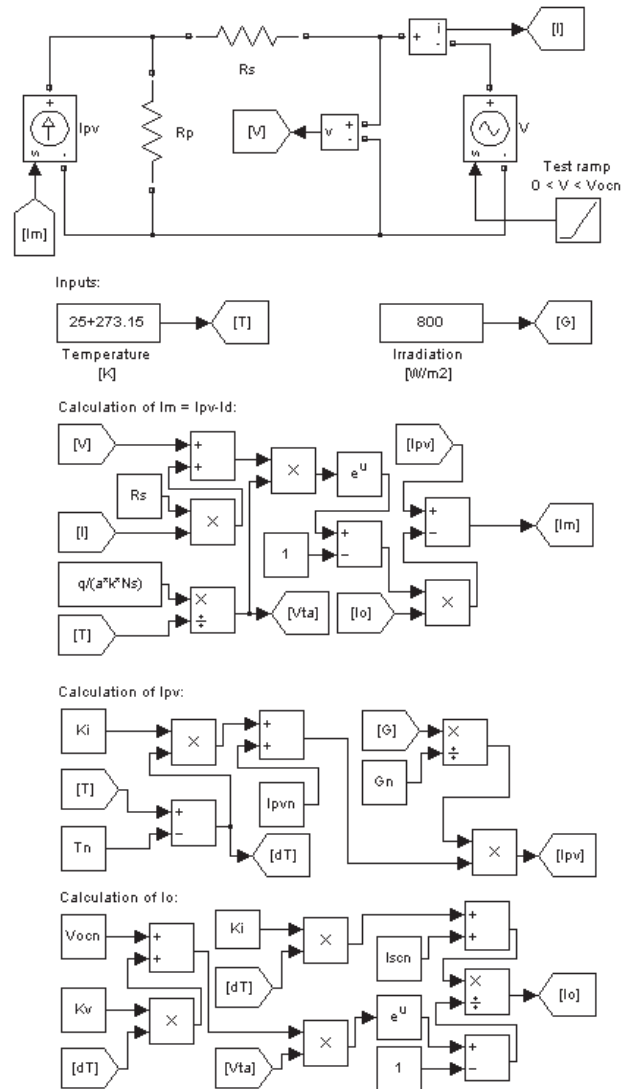

Fig. 17. Photovoltaic circuit model built with MATLAB/SIMULINK.

voltage/temperature coefficients. This paper has proposed an effective and straightforward method to fit the mathematical I-V curve to the three (V, I) *remarkable points* without the need to guess or to estimate any other parameters except the diode constant a. This paper has proposed a closed solution for the problem of finding the parameters of the single-diode model equation of a practical photovoltaic array. Other authors have tried to propose single-diode models and meth-
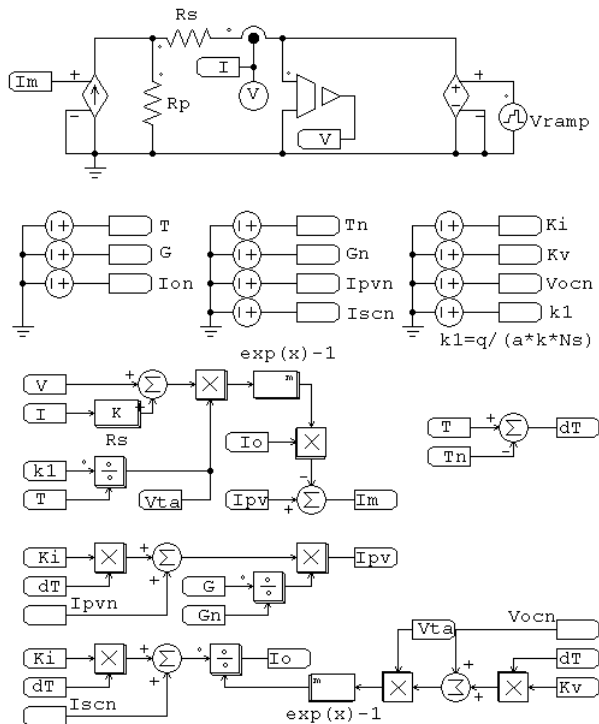
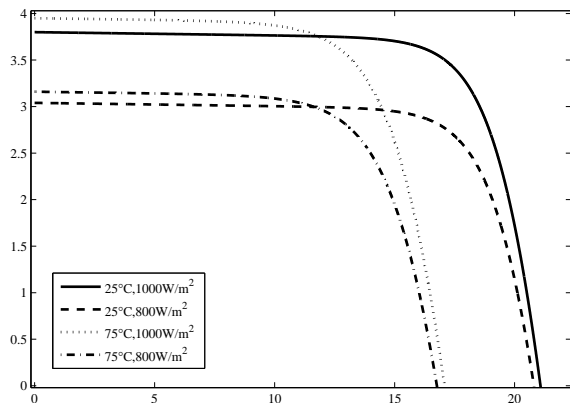Fig. 18.   Photovoltaic circuit model built with PSIM.

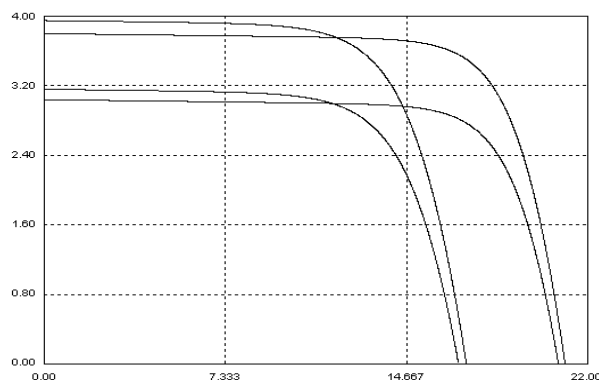Fig. 19.   *I-V* curves of the model simulated with MATLAB/SIMULINK.

Fig. 20.   *I-V* curves of the model simulated with PSIM.

ods for estimating the model parameters, but these methods always require visually fitting the mathematical curve to the *I-V* points and/or graphically extracting the slope of the *I-V* curve at a given point and/or successively solving and adjusting the model in a trial and error process. Some authors have proposed indirect methods to adjust the *I-V* curve through artificial intelligence [15], [44]–[46] and interpolation techniques [25]. Although interesting, such methods are not very practical and are unnecessarily complicated and require more computational effort than it would be expected for this problem. Moreover, frequently in these models R_s and R_p are neglected or treated as independent parameters, which is not true if one wish to correctly adjust the model so that the maximum power of the model is equal to the maximum power of the practical array.

An equation to express the dependence of the diode saturation current I_0 on the temperature was proposed and used in the model. The results obtained in the modeling of two practical photovoltaic arrays have demonstrated that the equation is effective and permits to exactly adjust the *I-V* curve at the open-circuit voltages at temperatures different of the nominal.

Moreover, the assumption $I_{pv} \approx I_{sc}$ used in most of previous works on photovoltaic modeling was replaced in this method by a relation between I_{pv} and I_{sc} based on the series and parallel resistances. The proposed iterative method for solving the unknown parameters of the *I-V* equation allows to determine the value of I_{pv}, which is different of I_{sc}.

This paper has presented in details the equations that constitute the single-diode photovoltaic *I-V* model and the algorithm necessary to obtain the parameters of the equation. In order to show the practical use of the proposed modeling method this paper has presented two circuit models that can be used to simulate photovoltaic arrays with circuit simulators.

This paper provides the reader with all necessary information to easily develop a single-diode photovoltaic array model for analyzing and simulating a photovoltaic array. Programs and ready-to-use circuit models are available for download at: http://sites.google.com/site/mvillalva/pvmodel.

APPENDIX - ASSOCIATION OF PV ARRAYS

In the previous sections this paper has dealt with the modeling and simulation of photovoltaic arrays that are single panels or modules composed of several interconnected basic photovoltaic cells. Large arrays composed of several panels may be modeled in the same way, provided that the equivalent parameters (short-circuit current, open-circuit voltage) are properly inserted in the modeling process. As a result, the equivalent parameters (resistances, currents, etc) of the association are obtained. Generally experimental data are available only for commercial low-power modules and this is the reason why this paper has chosen to deal with small arrays. The term array has been used throughout this paper to mean small commercial photovoltaic modules or panels. This appendix shows how to model and simulate large arrays composed of several series or parallel modules. Here, unlike in the rest of this paper, module and array have distinct meanings.
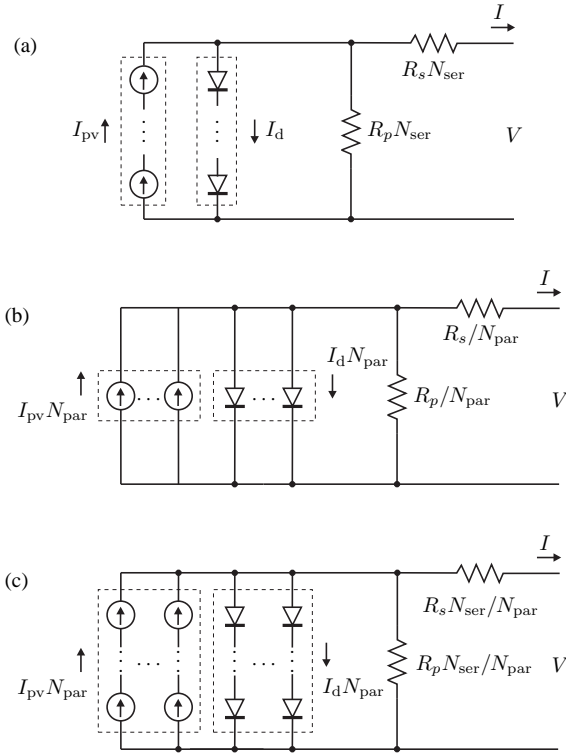
Fig. 21. (a) Array of N_{ser} modules connected in series, (b) Array of N_{par} modules connected in parallel, and (c) array composed of N_{ser} x N_{par} modules.

Fig. 22. Model circuit of array composed of N_{ser} x N_{par} modules.

The photovoltaic array can be simulated with the modified I-V equation (12). The simulation circuit presented previously must be modified according to the number of associated modules. The N_{ser} and N_{par} indexes must be inserted in the model, respecting equation (12), as shown in Fig. 22.

Fig. 21a shows an array composed of several identic modules connected in series. The output voltage is increased proportionately to N_{ser} and the currents remain unchanged. The equivalent series and parallel resistances are directly proportional to the number of modules.

Fig. 21b shows an array composed of several identic modules connected in parallel. The association provides increased output current and the output voltage is unchanged. The equivalent series and parallel resistances are inversely proportional to the number of parallel modules.

Fig. 21c shows a photovoltaic array composed of several modules connected in series and parallel. In this case the equivalent resistances depend on the number of series and parallel connections.

For any given array formed by N_{ser} x N_{par} identic modules the following equivalent I-V equation is valid:

$$I = I_{\text{pv}}N_{\text{par}} - I_0 N_{\text{par}}\left[\exp\left(\frac{V + R_{\text{s}}\left(\dfrac{N_{\text{ser}}}{N_{\text{par}}}\right)I}{V_{\text{t}}aN_{\text{ser}}}\right) - 1\right] - \frac{V + R_{\text{s}}\left(\dfrac{N_{\text{ser}}}{N_{\text{par}}}\right)I}{R_{\text{p}}\left(\dfrac{N_{\text{ser}}}{N_{\text{par}}}\right)}$$

(12)

where I_{pv}, I_0, R_{s}, R_{p}, and V_{t} are parameters of individual modules. Please notice that N_{s} (the number of elementary series cells of the individual photovoltaic module) used in the preceding sections is different of N_{ser}.
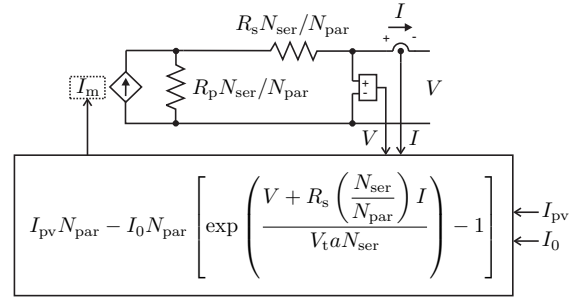
REFERENCES

[1] H. S. Rauschenbach. *Solar cell array design handbook.* Van Nostrand Reinhold, 1980.

[2] J. A. Gow and C. D. Manning. Development of a photovoltaic array model for use in power-electronics simulation studies. *Electric Power Applications, IEE Proceedings*, 146(2):193–200, 1999.

[3] J. A. Gow and C. D. Manning. Development of a model for photovoltaic arrays suitable for use in simulation studies of solar energy conversion systems. In *Proc. 6th International Conference on Power Electronics and Variable Speed Drives*, p. 69–74, 1996.

[4] N. Pongratananukul and T. Kasparis. Tool for automated simulation of solar arrays using general-purpose simulators. In *Proc. IEEE Workshop on Computers in Power Electronics*, p. 10–14, 2004.

[5] S. Chowdhury, G. A. Taylor, S. P. Chowdhury, A. K. Saha, and Y. H. Song. Modelling, simulation and performance analysis of a PV array in an embedded environment. In *Proc. 42nd International Universities Power Engineering Conference, UPEC*, p. 781–785, 2007.

[6] J. Hyvarinen and J. Karila. New analysis method for crystalline silicon cells. In *Proc. 3rd World Conference on Photovoltaic Energy Conversion*, v. 2, p. 1521–1524, 2003.

[7] Kensuke Nishioka, Nobuhiro Sakitani, Yukiharu Uraoka, and Takashi Fuyuki. Analysis of multicrystalline silicon solar cells by modified 3-diode equivalent circuit model taking leakage current through periphery into consideration. *Solar Energy Materials and Solar Cells*, 91(13):1222–1227, 2007.

[8] C. Carrero, J. Amador, and S. Arnaltes. A single procedure for helping PV designers to select silicon PV module and evaluate the loss resistances. *Renewable Energy*, 2007.

[9] E. Koutroulis, K. Kalaitzakis, and V. Tzitzilonis. Development of a FPGA-based system for real-time simulation of photovoltaic modules. *Microelectronics Journal*, 2008.

[10] G. E. Ahmad, H. M. S. Hussein, and H. H. El-Ghetany. Theoretical analysis and experimental verification of PV modules. *Renewable Energy*, 28(8):1159–1168, 2003.

[11] Geoff Walker. Evaluating MPPT converter topologies using a matlab PV model. *Journal of Electrical & Electronics Engineering, Australia*, 21(1), 2001.

[12] M. Veerachary. PSIM circuit-oriented simulator model for the nonlinear photovoltaic sources. *IEEE Transactions on Aerospace and Electronic Systems*, 42(2):735–740, April 2006.

[13] Ali Naci Celik and NasIr Acikgoz. Modelling and experimental verification of the operating current of monocrystalline photovoltaic modules using four- and five-parameter models. *Applied Energy*, 84(1):1–15, January 2007.

[14] Yeong-Chau Kuo, Tsorng-Juu Liang, and Jiann-Fuh Chen. Novel maximum-power-point-tracking controller for photovoltaic energy conversion system. *IEEE Transactions on Industrial Electronics*, 48(3):594–601, June 2001.

[15] M. T. Elhagry, A. A. T. Elkousy, M. B. Saleh, T. F. Elshatter, and E. M. Abou-Elzahab. Fuzzy modeling of photovoltaic panel equivalent circuit. In *Proc. 40th Midwest Symposium on Circuits and Systems*, v. 1, p. 60–63, August 1997.

[16] Shengyi Liu and R. A. Dougal. Dynamic multiphysics model for solar array. *IEEE Transactions on Energy Conversion*, 17(2):285–294, 2002.

[17] Weidong Xiao, W. G. Dunford, and A. Capel. A novel modeling method for photovoltaic cells. In *Proc. IEEE 35th Annual Power Electronics Specialists Conference, PESC*, v. 3, p. 1950–1956, 2004.

[18] Y. Yusof, S. H. Sayuti, M. Abdul Latif, and M. Z. C. Wanik. Modeling and simulation of maximum power point tracker for photovoltaic system. In *Proc. National Power and Energy Conference, PECon*, p. 88–93, 2004.

[19] D. Sera, R. Teodorescu, and P. Rodriguez. PV panel model based on datasheet values. In *Proc. IEEE International Symposium on Industrial Electronics, ISIE*, p. 2392–2396, 2007.

[20] M. A. Vitorino, L. V. Hartmann, A. M. N. Lima, and M. B. R. Correa. Using the model of the solar cell for determining the maximum power point of photovoltaic systems. In *Proc. European Conference on Power Electronics and Applications*, p. 1–10, 2007.

[21] D. Dondi, D. Brunelli, L. Benini, P. Pavan, A. Bertacchini, and L. Larcher. Photovoltaic cell modeling for solar energy powered sensor networks. In *Proc. 2nd International Workshop on Advances in Sensors and Interface, IWASI*, p. 1–6, 2007.

[22] H. Patel and V. Agarwal. MATLAB-based modeling to study the effects of partial shading on PV array characteristics. *IEEE Transactions on Energy Conversion*, 23(1):302–310, 2008.

[23] Wang Yi-Bo, Wu Chun-Sheng, Liao Hua, and Xu Hong-Hua. Steady-state model and power flow analysis of grid-connected photovoltaic power system. In *Proc. IEEE International Conference on Industrial Technology, ICIT*, p. 1–6, 2008.

[24] France Lasnier and Tony Gan Ang. *Photovoltaic engineering handbook*. Adam Hilger, 1990.

[25] K. Khouzam, C. Khoon Ly, C.and Koh, and Poo Yong Ng. Simulation and real-time modelling of space photovoltaic systems. In *IEEE 1st World Conference on Photovoltaic Energy Conversion, Conference Record of the 24th IEEE Photovoltaic Specialists Conference*, v. 2, p. 2038–2041, 1994.

[26] M. C. Glass. Improved solar array power point model with SPICE realization. In *Proc. 31st Intersociety Energy Conversion Engineering Conference, IECEC*, v. 1, p. 286–291, August 1996.

[27] I. H. Altas and A. M. Sharaf. A photovoltaic array simulation model for matlab-simulink GUI environment. In *Proc. International Conference on Clean Electrical Power ,ICCEP*, p. 341–345, 2007.

[28] E. Matagne, R. Chenni, and R. El Bachtiri. A photovoltaic cell model based on nominal data only. In *Proc. International Conference on Power Engineering, Energy and Electrical Drives, POWERENG*, p. 562–565, 2007.

[29] Yun Tiam Tan, D. S. Kirschen, and N. Jenkins. A model of PV generation suitable for stability analysis. *IEEE Transactions on Energy Conversion*, 19(4):748–755, 2004.

[30] A. Kajihara and A. T. Harakawa. Model of photovoltaic cell circuits under partial shading. In *Proc. IEEE International Conference on Industrial Technology, ICIT*, p. 866–870, 2005.

[31] N. D. Benavides and P. L. Chapman. Modeling the effect of voltage ripple on the power output of photovoltaic modules. *IEEE Transactions on Industrial Electronics*, 55(7):2638–2643, 2008.

[32] W. De Soto, S. A. Klein, and W. A. Beckman. Improvement and validation of a model for photovoltaic array performance. *Solar Energy*, 80(1):78–88, January 2006.

[33] Q. Kou, S. A. Klein, and W. A. Beckman. A method for estimating the long-term performance of direct-coupled PV pumping systems. *Solar Energy*, 64(1-3):33–40, September 1998.

[34] A. Driesse, S. Harrison, and P. Jain. Evaluating the effectiveness of maximum power point tracking methods in photovoltaic power systems using array performance models. In *Proc. IEEE Power Electronics Specialists Conference, PESC*, p. 145–151, 2007.

[35] R. A. Messenger and J. Ventre. *Photovoltaic systems engineering*. CRC Press, 2004.

[36] F. Nakanishi, T. Ikegami, K. Ebihara, S. Kuriyama, and Y. Shiota. Modeling and operation of a 10 kW photovoltaic power generator using equivalent electric circuit method. In *Conference Record of the 28th IEEE Photovoltaic Specialists Conference*, p. 1703–1706, September 2000.

[37] J. Crispim, M. Carreira, and R. Castro. Validation of photovoltaic electrical models against manufacturers data and experimental results. In *Proc. International*

Conference on Power Engineering, Energy and Electrical Drives, POWERENG, p. 556–561, 2007.

[38] K.H. Hussein, I. Muta, T. Hoshino, and M. Osakada. Maximum photovoltaic power tracking: an algorithm for rapidly changing atmospheric conditions. In *Generation, Transmission and Distribution, IEE Proceedings-*, v. 142, p. 59–64, January 1995.

[39] E. I. Ortiz-Rivera and F. Z. Peng. Analytical model for a photovoltaic module using the electrical characteristics provided by the manufacturer data sheet. In *Proc. IEEE 36th Power Electronics Specialists Conference, PESC*, p. 2087–2091, 2005.

[40] KC200GT high efficiency multicrystal photovoltaic module datasheet.

[41] Solarex MSX60 and MSX64 solar arrays datasheet, 1998.

[42] M. M. Casaro and D. C. Martins. Modelo de arranjo fotovoltaico destinado a análises em eletrônica de potência. *Revista Eletrônica de Potência, Sociedade Brasileira de Eletrônica de Potência (SOBRAEP)*, 13(3):141–146, 2008.

[43] R. C. Campbell. A circuit-based photovoltaic array model for power system studies. In *Proc. 39th North American Power Symposium, NAPS*, p. 97–101, 2007.

[44] Th. F. Elshatter, M. T. Elhagry, E. M. Abou-Elzahab, and A. A. T. Elkousy. Fuzzy modeling of photovoltaic panel equivalent circuit. In *Conference Record of the 28th IEEE Photovoltaic Specialists Conference*, p. 1656–1659, 2000.

[45] M. Balzani and A. Reatti. Neural network based model of a PV array for the optimum performance of PV system. In *Proc. PhD Research in Microelectronics and Electronics*, v. 2, p. 123–126, 2005.

[46] H. Mekki, A. Mellit, H. Salhi, and B. Khaled. Modeling and simulation of photovoltaic panel based on artificial neural networks and VHDL-language. In *Proc. 14th IEEE International Conference on Electronics, Circuits and Systems, ICECS*, p. 58–61, 2007.

BIOGRAPHIES

Marcelo Gradella Villalva was born in Campinas, São Paulo, Brazil, in 1978. He received the BSc (2002) and MSc (2005) in Electrical Engineering from the University of Campinas (UNICAMP), Brazil, where he is currently working towards the PhD degree. His research interests are active filters, modeling and control of electronic converters, photovoltaic energy systems, distributed generation and artificial intelligence applied to power electronics.

Jonas Rafael Gazoli was born in Americana, São Paulo, Brazil, in 1983. He received in 2008 the BSc in Electrical Engineering from the University of Campinas (UNICAMP), Brazil, where he is currently working towards the MSc degree. His research interests include power electronics for solar energy conversion and control strategies for electrical drives.

Ernesto Ruppert Filho was born in Jundiaí, São Paulo, Brazil. He received from the University of Campinas (UNICAMP), Brazil, the BSc, MSc and PhD degrees in Electrical Engineering in 1971, 1974, and 1982, respectively. During his professional life he has worked in Brazil and abroad as a project engineer and/or consultant for several large companies such as Itaipu, Petrobras, General Electric, Alstom, Copel, CPFL, and Elektro. He has been with the University of Campinas (UNICAMP) since 1972 as a professor and researcher. He is currently a full professor and coordinates several research projects with private companies and public institutions in Brazil. His research interests are power electronics, superconductor current limiters, electrical power systems, distributed generation, electric machines and motor drives. He has published many technical papers in international journals and conferences and has advised several MSc and PhD theses along his career.